The neuron-specific interleukin-1 receptor accessory protein is required for homeostatic sleep and sleep responses to influenza viral challenge in mice

Christopher J. Davis[*,1], **Danielle Dunbrasky**[1], **Marcella Oonk**[1], **Ping Taishi**[1], **Mark R. Opp**[2], and **James M. Krueger**[1]

[1]College of Medical Sciences and the Sleep and Performance Research Center, Washington State University – Spokane, Spokane, WA 99210

[2] Department of Anesthesiology & Pain Medicine, University of Washington, Seattle, WA 98104

Abstract

Interleukin-1β, (IL1) is involved in sleep regulation and sleep responses induced by influenza virus. The IL1 receptor accessory protein (AcP) and an alternatively spliced isoform of AcP found primarily in neurons, AcPb, form part of the IL1 signaling complex. IL1-induced sleep responses depend on injection time. In rat cortex, both IL1 mRNA and AcPb mRNA peak at Zeitgeber Time (ZT) 0 then decline over the daylight hours. Sleep deprivation enhances cortical IL1 mRNA and AcPb mRNA levels, but not AcP mRNA. We used wild type (WT) and AcPb knockout (KO) mice and performed sleep deprivation between ZT10-20 or between ZT22-8 based on the time of day expression profiles of AcPb and IL1. We hypothesized that the magnitude of the responses to sleep loss would be strain- and time of day-dependent. In WT mice, NREMS and REMS rebounds occurred regardless of when they were deprived of sleep. In contrast, when AcPbKO mice were sleep deprived from ZT10-20 NREMS and REMS rebounds were absent. The AcPbKO mice expressed sleep rebound if sleep loss occurred from ZT22-8 although the NREMS responses were not as robust as those that occurred in WT mice. We also challenged mice with intranasal H1N1 influenza virus. WT mice exhibited the expected enhanced sleep responses. In contrast, the AcPbKO mice had less sleep after influenza challenge compared to their own baseline values and compared to WT mice. Body temperature and locomotor activity responses after viral challenge were lower and mortality was higher in AcPbKO than in WT mice. We conclude that neuron-specific AcPb plays a critical role in host defenses and sleep homeostasis.

Keywords

cytokine; H1N1; recuperation; PR8; sleep deprivation; mouse

[*]Corresponding Author: Christopher J. Davis, P.O. Box 1495, Spokane, WA 99202, Phone No. 509-358-7820, cjdavis@wsu.edu.

Introduction

Interleukin-1β (IL1) is part of the molecular sleep homeostat in health and disease (Krueger 2008; Imeri and Opp 2009). Injection of exogenous IL1 enhances non-rapid eye movement sleep (NREMS) in multiple species. At low somnogenic doses IL1 has little effect on rapid eye movement sleep (REMS) or body temperature. Higher doses can inhibit both NREMS and REMS and induce fever (Opp et al 1991). Inhibition of IL1 using anti-IL1 antibodies, or a soluble IL1 receptor, or the IL1 receptor antagonist reduces the time spent in NREMS (reviewed Krueger 2008). Further, mice lacking the type I IL1 receptor have less spontaneous NREMS and REMS during the night hours. These mice also lack the ability to generate sleep responses to exogenous IL1 (Fang et al 1998). Brain levels of IL1 mRNA vary with the time of day with highest levels occurring at Zeitgeber Time (ZT) 0, the beginning of the sleep period (Taishi et al 1997; 2012). Inhibiting caspase-1, the enzyme cleaves the pro-form of IL1 to produce mature IL1, reduces spontaneous NREMS and attenuates sleep responses to lipopolysaccharide (LPS; Imeri et al 2006). Lastly, after sleep loss and infectious challenge, sleep and brain levels of IL1 mRNA or IL1 protein are enhanced (Taishi et al 1998; Leyva-Grado et al 2009; reviewed Imeri and Opp 2009).

The IL1 receptor accessory protein (IL1R AcP) binds to the IL1/IL1 receptor complex triggering a biochemical signaling cascade. An alternatively-spliced isoform of the IL1R AcP, the neuron-specific IL1R AcP, called AcPb, is expressed predominately in brain (Smith et al 2009; Huang et al 2011; Taishi et al 2012). Previously we showed that in response to sleep loss, AcPb mRNA, but not AcP mRNA, is up-regulated in brain (Taishi et al 1998; 2012). Maximum spontaneous levels of brain AcPb mRNA occur at ZT0, as do IL1 mRNA levels. Further, exogenous somnogenic doses of IL1 enhance brain AcPb mRNA, but not AcP mRNA. These results collectively suggest the involvement of AcPb in spontaneous sleep regulation and in the expression of sleep responses induced by sleep loss or microbial challenge.

Influenza A/PR/8/34 (PR8) is an H1N1 human strain adapted to replicate in mice. PR8 is found in the brain olfactory bulb (OB) within 4 h post-intranasal instillation (PI) (Majde et al 2007). Pro-inflammatory cytokine mRNAs, including IL1, are elevated in the OB at 15 h PI when the mice become overtly ill when a high dose of virus is used (Majde et al 2007). Virus appears to be restricted to glia of the outer layers of the OB, but the number of IL1-expressing neurons increases in olfactory and autonomic pathways with projections from the olfactory system (Leyva-Grado et al 2009). Illness onset correlates with increased numbers of IL1-expressing neurons in the hypothalamus, a sleep regulatory area (Leyva-Grado et al 2009).

In this study, we determined the sleep responses of wild type (WT) mice and mice lacking the AcPb (AcPb knockout [KO]) mice to sleep deprivation and in separate experiments sleep and sickness responses to influenza virus challenge. We report that AcPbKO mice have attenuated sleep responses after sleep loss and virus challenge.

Materials and Methods

Animals

Male C57BL/6 mice (control strain) were from Jackson Laboratories, (Bar Harbor, ME) and male IL1 receptor AcPb knockout (KO) mice (experimental strain), were provided by Amgen (Seattle, WA) and bred for 5-7 generations at Washington State University, were used in these studies. Subsequent homozygote offspring were used in the experiments. Mice were sleep deprived or infected at 2-3 months of age. Breeding mice were maintained on a 14:10 h light-dark cycle and experimental mice were on a 12:12 light-dark cycle (light onset = ZT0). All mice were genotyped from tail snips by Transnetyx (Cordova, TN). Mice were maintained in plastic filter-top cages at 23-24° C and during recordings in sound-attenuated environmental chambers. Food and water were available *ad libitum*. All animal procedures were approved by the Washington State University Animal Care and Use Committee and conformed to National Institutes of Health guidelines.

Mice used for polysomnographic analyses were anesthetized with an intraperitoneal (ip) injection of ketamine-xylazine (87 and 13 mg/kg, respectively) for surgical implantation of electroencephalographic (EEG) electrodes over the right and left parietal cortices and over the cerebellum, which acted as a ground as previously described (Taishi et al 2012). In addition, a stainless steel electromyogram (EMG) electrode was placed in the dorsal neck muscles. The electrodes were fixed on the head with dental cement. Mice were allowed at least 7 days to recover from the surgical procedure and to acclimate to the tethered polysomnographic cables. In an independent experiment, biotelemetry transmitters (Minimitter, Bend, OR) were chemically sterilized and implanted intraperitoneally via the anesthesia regimen reported above. Mice were allowed to recover for at least one week after surgery and housed individually in cages placed atop ER-4000 receiver plates.

Polysomnographic Recording and Analyses

Polysomnographic recording cables connected the head electrodes to commutators that were in turn led to amplifiers. The analog EEG and EMG signals from the amplifiers were converted to digital signals (128 Hz sampling rate) and recorded. EEG signals were filtered below 0.1 Hz and above 100 Hz with a 60 Hz notch filter. EEG analyses were conducted using Sleep Sign Software (Kissei Comtec Co., Ltd, Japan). Vigilance states including wakefulness, NREMS, and rapid-eye movement sleep (REMS) were manually determined off-line in 10 s epochs as described previously (Taishi et al 2012). Briefly, NREMS was characterized by high-amplitude EEG signals and low EMG activity. REMS was identified by regular low-amplitude EEG and minimal EMG activity. Wakefulness was determined when the signal exhibited low amplitude fast EEG and high EMG activity. Time spent in REMS or NREMS, the duration and frequency of REMS or NREMS episodes were calculated in 2 h or 12 h time blocks. After artifact exclusion from individual NREMS-scored epochs, EEG signals were analyzed by fast Fourier transformation using a Hanning window. NREMS EEG slow wave activity (SWA; 0.5-4 Hz) was determined within each epoch. The means of the 24 h EEG SWA control values for each mouse were used as a reference value to normalize the data for both the control and experimental treatment days as previously described (Krueger et al 2010). EEG SWA values for each animal were

determined for 2 h or 12 h time bins and presented as a percentage of the 24 h baseline values. In addition, power spectra in the 0-20 Hz range were extracted for the first 4 h post-SD or the 12 h light or dark period. These data were normalized using a 24 h average of the NREMS-scored 0-20 Hz spectral content comprised of 1 Hz bin sums from 2 h or 12 h periods of individual mice.

Sleep Deprivation and Recovery

Experiment 1a: SD ZT22-8—Age-matched mice (n=8/strain) were placed in sound attenuated recording chambers and acclimated to the headstage and cables for 2 days prior to recording a 24 h baseline ZT8-8. Then mice were subjected to gentle handling SD for a 10 h period from ZT22-8 as previously described (Taishi et al 2012). The 10 h SD periods in Experiments 1a and 1b were selected based on the sleep deficits in IL1 type I receptor KO mice which occur from ZT12-20 (Fang et al 1998) and the differences in the timing of IL1 and AcPb cortical gene expressions (Taishi et al 2012). EEG recordings continued for 24 h after the end of SD to document the recovery sleep/wake responses. Two mice were excluded due to the loss of headcap interface and one due to the detection of seizure activity during manual scoring. Thus, six WT mice and seven AcPbKO mice were used in subsequent sleep analyses.

Experiment 1b: SD ZT10-20—Mice (n=12/strain) were acclimated and baseline recorded as above, except that the 24 h baseline was recorded from ZT20-20. In this study, gentle-handling SD occurred from ZT10-20. EEG recordings ensued for 24 h after SD. Whereas, the previous ZT22-8 SD study was completed in two rounds, this study used a third round to confirm by replication the absence of rebound sleep to ZT10-20 SD, reported hereafter. Two WT mice were excluded the study due to the loss of a headcap interface. Accordingly, data from ten WT and 12 AcPbKO mice were analyzed.

Virus Purification and Titration—A mouse-adapted H1N1 A/Puerto Rico/8/34 H1N1 (PR8) influenza virus (lot # 3X010621) was suspended in pyrogen-free allantoic fluid (Specific Pathogen-Free Avian Supply, North Franklin, CT) and purified by ultracentrifugation sucrose-gradient sedimentation as previously described (Grimm et al 2007; Majde et al 2007). The virus was diluted to a protein concentration of 200 μg/ml, aliquoted, frozen on dry ice, and stored at −80°C. A standard hemagglutination assay with two-fold dilutions of purified PR8 (10 μl) mixed with 50 μl chicken red blood cells and incubated at room temperature for 30 min yielded 1×10^7 virus particles/ml. Samples were tested for endotoxin using a Limulus lysate gel-clot assay (Biowhittaker, Walkersville, MD); endotoxin was below detection levels. Additionally, the purified virus was negative for mycoplasma and acholeplasma contamination as determined by nested PCR. In Madin-Darby canine kidney cells (MDCK; ATCC, Manassas, VA), viral titrations were assessed and expressed as median tissue culture infectious doses ($TCID_{50}$) as described elsewhere (Grimm et al 2007). The starting titer of purified PR8 virus was 2.5×10^4 $TCID_{50}$/ml.

Body Temperature and Locomotor Activity Recording and Analyses—
Telemetric signals were recorded at 6 min intervals, and data points derived from those values were averaged over 6 h bins for body temperature and activity. Activity counts for

every 6 h and from each mouse were normalized by dividing the 6 h value by its total 24 h activity count and are expressed as a percent of baseline. Baseline was recorded for 24 hours beginning at ZT0 and continued for 9 days. Morbidity was visually determined by daily examination of online temperature graphs and the criteria established for euthanization was mice showing < 31°C for 12 h.

Influenza Virus Challenge

Experiment 2a: PR8 Infection and Polysomnography—WT (n=13) or AcPbKO (n=7) mice were acclimated to the experimental chambers and instrumentation for 2 days before recording a 24 h baseline ZT0-0. Then each mouse received 12.5 $TCID_{50}$ of purified mouse-adapted PR8 influenza virus. The live virus delivery occurred by intranasal instillation of 50 μL of purified PR8, 25 μL per nostril, under 20% isoflurane/80% polyethylene glycol (isoflurane-PEG) anesthesia. The intranasal virus was given within 1 h of light onset (ZT0-1). After viral challenge, mice were placed back in their recording chambers and EEG and EMG were recorded for the next 8 days. Three AcPbKO mice were omitted due to loss of headcap, so 13 WT mice and 7 AcPbKO mice were included for data analyses. Data attrition on PI Day 4 was due to a failed UPS battery backup for the recording system. Attrition on subsequent recording days occurred when an animal died or was euthanized after succumbing to the infection.

Experiment 2b: PR8 Infection, Body Temperature and Locomotor Activity—
WT (n=11) or AcPbKO (n=11) mice were acclimated to the recording chamber for at least one week after surgery before recording a 24 h baseline for temperature and activity. Next, mice were infected using the same technique and dose as above, returned to their cages and recordings ensued for the next 9 days.

Statistical Analyses—In Experiments 1a and 1b, mixed three-way ANOVAs, performed in SPSS v17.0, were used to assess factors of strain (WT vs. AcPbKO), treatment (baseline vs. post-SD), and time (in 2 h bins) for the dependent variables: time spent in NREMS or REMS, number of bouts and bout lengths of REMS and NREMS, in addition to NREMS EEG SWA. A three-way mixed ANOVA was used to compare NREMS spectral power with repeated measures of spectral frequency (0-20 Hz), treatment, and strain as an independent factor. A Huynh-Feldt adjustment was used to mitigate sphericity violations of the repeated measures, however the unadjusted degrees of freedom are reported for clarity. In Experiment 2a, two-way ANOVAs (strain and treatment) were run on light and dark periods separately using differences from baseline values for each of the response variables reported above, except for the power spectra analyses which were performed as above. *A priori* comparisons of baseline vs. post PI days were performed when a significant treatment effect was detected on the raw or normalized values, not difference scores. Temperature and activity data were analyzed with a mixed three-way ANOVA in 6 h bins in Experiment 2b. Post hoc comparisons were made using independent or paired *t*-tests when appropriate. In Experiment 2b the alpha level of the t-tests was adjusted to $p < 0.01$ to account for additional comparisons incurred with 6 h bins over 10 days, for all other analyses $p < 0.05$ was considered statistically significant.

Results

Sleep Deprivation and Recovery

Experiment 1a: SD ZT22-8—After 10 h of SD from ZT22-8, WT mice showed the expected NREMS rebound after SD [Treatment × Time: $F_{(11,121)}$=5.62, p<0.001]. The rebound was evident in the remaining 4 h light period immediately after SD (ZT8-12) within which WT mice had an additional 22 min of NREMS over their baseline values (Fig 1A). The AcPbKO mice had 12 min of extra NREMS during the initial 4 h after SD, but this increase was not significant (Fig 1A). The NREMS rebound continued during the subsequent dark period (ZT12-0) in both strains with 50 min extra NREMS in WT mice [t-test, p< .05] and 57 min additional NREMS in AcPbKO mice [t-test, p< .001], each compared with their respective baseline values (data not shown). Compared to baseline the average duration of NREMS epochs increased during ZT8-12 after SD [Treatment × Time: $F_{(11,121)}$=2.96, p<0.01] by an average of 62 s in WT mice and 78 s in AcPbKO mice (Fig 1D), whereas the number of NREMS epochs decreased [Treatment × Time: $F_{(11,121)}$=6.98, p<0.001; data not shown] by an average of 6.5 in WT and 12.5 in AcPbKO mice. The differences between strains with either NREMS epoch duration or frequency were not significant.

REMS in WT mice roughly doubled in the first 4 h post-SD (ZT8-12) with respect to baseline levels [Treatment × Time: $F_{(11,121)}$=8.34, p<0.001], with a cumulative increase of 13 min (Fig 1B). Compared to WT mice, the REMS rebound in AcPbKO mice was significantly attenuated with 9 min of extra REMS above their baseline values during ZT8-12 (Fig 1B). The REMS rebound continued in both strains into the following dark period (ZT12-0) [Strain × Time: $F_{(11,121)}$=1.90, p<0.05; data not shown] with 11 min increase from baseline in WT mice [t-test, p<0.01] and 12 min in AcPbKO mice [t-test, p<0.01]. During ZT8-12, the 4 h immediately after SD, the average REMS epoch length increased compared to baseline [Treatment × Time: $F_{(11,121)}$=2.85, p<0.01] by an average of 30 s in WT mice and 16 s in AcPbKO mice (Fig 1E), and the number of REMS epochs also increased [Treatment × Time: $F_{(11,121)}$=4.19, p<0.001; data not shown] by an average of 2.5 in WT and 1.0 in AcPbKO mice. The strain differences for REMS epoch duration and frequency were significant [Strain × Treatment: $F_{(11,121)}$=2.23, p<0.05, and $F_{(11,121)}$=2.37, p<0.05, respectively]. Further, there was a significant REMS epoch length decrease for AcPbKO mice during ZT8-10 as compared with WT mice. During the initial 4 h after SD (ZT8-12), WT and AcPbKO mice (Fig 1C) displayed the typical NREMS EEG SWA increase with respect to their respective baseline records [Treatment × Time: $F_{(11,99)}$=9.04, p<0.001]. In the subsequent dark period following SD (ZT12-0), both strains demonstrated a negative rebound as occurs in mice after SD and is characterized by delayed decrease in NREMS EEG SWA (data not shown). Spectral content of the NREMS EEG from the ZT8-12 periods was altered by SD [Treatment × Hz: $F_{(19,171)}$=33.06, p<0.001]. In WT mice, the increases in the 1-3 Hz band and decreases in the 5-6 and 6-7 Hz bands (Fig 1F). In AcPbKO mice, SD enhanced power in the 1-3 and 9-10 Hz ranges (Fig 1F). No significant differences between strains occurred for either NREMS EEG SWA or the power spectrum.

Experiment 1b: SD ZT10-20—WT mice subjected to SD from ZT10-20 had excess NREMS during the immediate subsequent 4 h, ZT20-24 (Fig 2A). In contrast, AcPbKO mice failed to produce a NREMS rebound in response to SD from ZT10-20 (Fig 2A); in fact they had 6 min less NREMS than their baseline values in the first 4 h after SD [Strain × Treatment × Time: $F_{(11,220)}=1.34$, $p<0.05$]. There was a significant difference in NREMS duration during ZT20-22 between strains (Fig 2A). In either strain, there were no NREMS increases during the subsequent post-SD light period (ZT0-12; data not shown). In the first 4 h after SD, NREMS epoch lengths increased by 20 s in WT mice and 25.5 s in AcPbKO mice [Treatment × Time: $F_{(11,220)}=2.36$, $p<0.05$], but only the values obtained during the first 2 h post-SD in WT were significant (Fig 2D). The number of NREMS epochs during ZT20-0 did not change in WT mice, and was reduced by 7.5 in AcPbKO mice [Treatment: $F_{(1,20)}=6.23$, $p<0.05$]. During the post-SD light period NREMS epoch lengths did not differ from respective baseline values. Moreover, no significant strain differences in NREMS epoch length or frequency were observed at any time block.

After SD from ZT10-20, REMS rebound occurred within the initial 4 h post-SD (ZT20-24) in WT mice [significant during ZT20-22; Fig 2B, Treatment × Time: $F_{(11,220)}=2.29$, $p<0.05$], whereas no significant rebound occurred in AcPbKO mice (Fig 2B). Further, the REMS rebound in WT mice persisted (data not shown), and was significant at ZT2-4, 10-12 and 12-14. Despite the reported treatment differences occurring within the strains, there were no significant strain effects in REMS durations. REMS epoch lengths increased [Strain × Treatment × Time: $F_{(11,220)}=1.94$, $p<0.05$] by 17.5 s in WT mice (significant between ZT20-22; Fig 2E) and 4.5 s in AcPbKO mice (significant between ZT22-0; Fig 2E) in the 4 h immediately after SD (ZT20-24), but did not differ from baseline in the subsequent light period (ZT0-12; data not shown). Finally, SD also increased REMS epoch frequency in WT mice but not in AcPbKO mice [Strain × Treatment × Time: $F_{(11,220)}=1.94$, $p<0.05$; data not shown].

Between ZT20-0, the 4 h dark period right after SD, NREMS EEG SWA was greater than baseline values in WT and AcPbKO mice [Fig 2C; Treatment × Time: $F_{(11,198)}=13.18$, $p<0.001$]. In both strains these effects were significant during the first 2 h (ZT20-22). Further, in AcPbKO mice a compensatory decrease in NREMS EEG SWA occurred during ZT10-12 (data not shown). During the 4 h post-SD periods, spectral content changed in both strains [Treatment × Hz: $F_{(19,342)}=11.66$, $p<0.001$]. In WT mice, power increased in the 1-20 Hz range (Fig 2F), whereas in AcPbKO mice, increases occurred in the 1-4 and 12-15 Hz bands after SD (Fig 2F). No statistically significant strain differences were found for either NREMS EEG SWA or the power spectrum.

Influenza Virus Challenge

Experiment 2a: Sleep responses to PR8 infection—The dose of influenza virus used in the current experiments was lower than the dose of the same virus preparation used in our prior work to allow a slower onset of morbidity and mortality; thus the effects of the virus on sleep took longer to manifest. Consistent with the literature, NREMS amounts in the dark increased following infection in WT mice [Fig 3A, Day: $F_{(3,40)}=2.94$, $p<0.05$]. For instance, on PI Day 8, WT mice had more NREMS during the 12 h dark period (ZT12-0)

compared to their own baseline values [t-test, p<0.01]. In contrast, the AcPbKO mice had less NREMS in the ZT12-0 period after viral challenge compared to WT mice [Fig 3C, Strain: $F_{(1,59)}$=7.66, p<0.01] on PI Day 8 [t-test; p<0.05], but the PI AcPbKO NREMS values were not different from the AcPbKO baseline values. Time in NREMS did not differ in either strain during the light period. After infection, there were significant changes between strains in the number and length of NREMS bouts that occurred during the light [Figs 3B and 3D, Strain: $F_{(1,59)}$=12.58, p<0.01; bout length not shown, Strain: $F_{(1,59)}$=17.58, p<0.01, respectively] and dark periods [Figs 3B and 3D; Strain: $F_{(1,59)}$=30.25, p<0.001; bout length not shown, Strain: $F_{(1,59)}$=7.28, p<0.01, respectively]. Although time in NREMS was not different during the light in either strain, on PI day 6, WT mice averaged 155.67 more NREMS bouts [t-test; p<0.05] with 31.8 s shorter bout duration [t-test, p<0.01] compared to AcPbKO mice, indicating that NREMS sleep was more fragmented in WT mice. This effect was even more apparent during the dark phase, when WT mice spent more time in NREMS. On PI day 6, WT mice had 256.8 more NREMS bouts [t-test, p<0.01] with 17.5 s less bout length [t-test, p<0.001] and on PI day 8 they had 155.2 more NREMS bouts [t-test, p<0.01] with a 16.4 s decrease in bout length [t-test, p<0.001] with respect to AcPbKO mice. While several statitically significant treatment changes were detected using t-tests on single PI days, non-significant factorial analyses disallowed such comparisons. Thus, treatment effects for light or dark periods are not reported for NREMS bout counts or bout lengths. Time spent in REMS decreased in WT mice during the light and dark periods as compared with their baseline amounts [Fig 3E, Day: $F_{(3,40)}$=9.51, p<0.001; Day: $F_{(3,40)}$=2.83, p=0.05, respectively]. On PI day 6, WT mice had 17.3 min less REMS during the light [t-test, p<0.05] and 6.1 min less REMS during the dark period [t-test, p<0.01]. Attenuated REMS in WT mice continued on PI day 8 with a 40.9 min reduction from baseline [t-test, p<0.001] during the light period and a 8.7 min decrease in REMS during the dark [t-test, p<0.01]. In AcPbKO mice treatment differences in REMS amounts were not detected during the light period, however REMS decreases from baseline were present in the dark period [Fig 3G, Day: $F_{(3,38)}$=3.30, p<0.05] with -10.2 min [t-test, p<0.01] and -11.01 min [t-test, p<0.01] on PI days 6 and 8, respectively. The suppressed REMS during the light period in WT mice following viral challenge was absent in AcPbKO mice [Strain: $F_{(1,59)}$=24.62, p<0.001] and significantly different on PI days 6 [t-test, p<0.05] and 8 [t-test, p<0.01]. During the dark period strain differences in REMS amounts were not statistically significant. The number of REMS bouts in WT mice decreased from baseline during the light and dark periods [Fig 3F, Day: $F_{(3,40)}$=10.12, p<0.001; Day: $F_{(3,40)}$=5.88, p=0.01, respectively] on the PI days 6 [t-test, p<0.05] and 8 [t-test, p<0.01] during the light and PI day 8 during the dark [t-test, p<0.01]. In AcPbKO mice REMS bout frequency was elevated from baseline during the light, but not dark, periods [Fig 3H] and strain differences were detected via a significant interaction effect [Strain × Day: $F_{(3,59)}$=4.11, p<0.05]. REMS bout lengths were not different from baseline on any specific day in either strain. However during the light period, WT mice had 29.2 [t-test, p<0.05] and 58.8 [t-test, p<0.001] fewer REMS bouts than AcPbKO mice on PI day 6 and 8, respectively. WT mice also had longer REMS bouts, than AcPbKO mice [not shown, Strain: $F_{(1,59)}$=18.69, p<0.001] on PI day 6 by 29.2 s [t-test, p<0.05; on PI day 8, t-test p=0.05]. Despite the increased bout durations in the dark, the decreased REMS amounts coupled with

fewer REMS bouts during the light and dark periods in WT mice, is consistent with the literature and indicate an atypical REMS response to viral challenge in AcPbKO mice.

Compared to WT mice (Fig 3I), AcPbKO mice (Fig 3K) had larger reductions of NREMS EEG SWA in the light and dark periods following viral challenge [Strain: $F_{(1,54)}=12.97$, $p<0.001$; Strain: $F_{(1,54)}=4.14$, $p<0.05$, respectively], but the changes were only significant on PI day 6 [t-tests, $p<0.05$ for light and dark periods] because both strains had their largest decreases on PI day 8. Although NREMS EEG SWA was significant different from baseline on specific PI days in AcPbKO, but not in WT mice, main effects of Day were not present in light or dark periods and therefore excluded.

In WT mice, EEG FFT spectral content in the higher frequency ranges was also affected [Fig 3J; Day: $F_{(4,70)}=3.61$, $p<0.05$] on PI Day 8; decreases in the 6-13 Hz and 6-16 Hz ranges for the light and dark periods, respectively. In AcPbKO mice on PI Day 8, reductions in EEG FFT power occurred in the 1-4 Hz and 6-7 Hz ranges during the light [Fig 3L, Day: $F_{(4,70)}=3.31$, $p<0.05$], but the decreases during the dark period were not statistically significant (not shown).

Experiment 2b: Temperature and activity responses to PR8 infection—The onset of hypothermia [Fig 4A, Strain $\times$ Day: $F_{(9,180)}=4.97$, $p<0.05$] and locomotor activity deficits [Fig 4B, Strain $\times$ Day: $F_{(9,180)}=2.85$, $p<0.05$] following infection were more severe in AcPbKO mice and were accompanied with higher mortality rates (Fig 4C). The strain differences for both sickness measures were apparent on PI day 3 and continued to varying degrees through PI day 9. For instance, on PI Day 8, WT mice showed a 2.02 °C reduction in temperature [Day: $F_{(1,10)}=12.86$, $p<0.01$] and a corresponding 58% decrement in activity [Day: $F_{(1,10)}=23.14$, $p<0.01$] from baseline. Comparatively, in AcPbKO mice, more dramatic decreases from baseline temperature [−3.96 °C; $F_{(1,10)}=71.63$, $p<0.001$] and activity [−80%; $F_{(1,10)}=15.82$, $p<0.001$] occured on PI Day 8.

Discussion

The AcPbKO mouse responses to SD indicate a substantive role for AcPb in sleep homeostasis regulation (Figs 1 and 2). Of particular interest is that NREMS rebound is absent in AcPbKO mice, but not in WT mice, following ZT10-20 SD. Although not statistically significant during the first 2 h after SD ($p=0.06$), AcPbKO mice sleep less than their own baseline control values after SD (Fig 2A) and lack a rebound in the 20 h thereafter as indicated by cumulatively summing of NREMS differences from baseline in the post-SD hours (e.g. ZT20-0, ZT20-4 etc.) never yields a positive number. Further, the loss of NREMS rebound is not substituted by REMS as the post-SD REMS increase is negligible (Fig 2B), nor is it compensated by higher sleep intensity in AcPbKO mice as evidenced by NREMS EEG SWA levels comparable to the levels observed in WT mice (Fig 2C). We conclude that AcPb plays a role in sleep homeostasis to the extent that it is required for sleep rebound after SD during ZT10-20.

The effects of SD between ZT10-20 are distinct from those following SD from ZT22-8 in their magnitude, timing and in AcPb mice the direction of effects on NREMS. Prior work

suggests multiple interactions with IL1 signaling and the circadian clock. Thus, in rats injection of IL1 during the dark enhances NREMS while the same dose given during light hours reduces NREMS (Opp et al 1991). SD has different effects on recovery sleep that are dependent upon when the sleep loss occurs in both rats (Tobler and Borbely 1986; Vyazovskiy et al 2007) and mice (Huber et al 2000; Franken et al 2001). Mice lacking the type I IL1 receptor have less spontaneous sleep during the night than WT mice, but not during the day (Fang et al 1998). IL1β and its receptors fluctuate across the day (Taishi et al 1997; 1998; 2012). Further, both IL1 and AcPb mRNAs are up-regulated by SD (Taishi et al 1998; 2012). Peak somatosensory AcPb mRNA and IL1 mRNA expressions occur at ZT0 although during the preceding dark hours, ZT12-0, the IL1 mRNA relative values decrease proportionally less than AcPb mRNA values whereas for the hours ZT0-8 AcPb values are less than IL1 values (Taishi et al 2012). Further, IL1 inhibits the expression of period 1, 2 and 3 via Clock-BMal1-induced activation of E-box regulatory elements (Cavadini et al 2007). Collectively such findings suggest IL1 signaling mechanisms interacting with circadian rhythm mechanisms manifest uniquely at different times of the day to affect sleep; current results are consistent with this conclusion.

There is a robust literature linking sleep and sleep loss to host defenses (reviewed Toth and Jhaveri 2003; Imeri and Opp 2009; Zielinski and Krueger 2011; Besedovsky et al 2012). Indeed, chronic sleep loss is associated with chronic inflammation; sleep loss-induced up-regulation of IL1 and other cytokines are involved in these inflammatory processes. A separate literature describes the relationships between infectious challenge, and the associated severe inflammation, and other inflammatory stimuli such as LPS and sleep responses as a component of host defenses (reviewed Majde and Krueger 2005). Current results suggest that AcPb is also a key component in sleep responses to inflammation to the extent that AcPbKO mice slept less following viral challenge and ultimately this correlated with higher morbidity and mortality. This finding is consistent with earlier work in rabbits showing a correlation between robust sleep responses to infectious challenge and lower morbidity (Toth et al 1993). Similar findings were reported in bacteria-infected *drosophila* that had less sleep rebound after sleep deprivation also had increased mortality rates (Kuo and Williams, 2014). These data directly support the link between sleep and innate immunity and overall health as shown here and in other reports (Toth and Jhaveri 2003; Imeri and Opp, 2009; Zielinski and Krueger 2011; Besedovsky et al 2012).

Severe influenza infection in mice is characterized by a precipitous reduction in body temperature (Wong et al 1997) together with a disappearance of circadian temperature rhythms (Conn et al 1995; Majde et al 2007). This is consistent with our sleep EEG and temperature patterns in WT mice (Figs 3A, 3E & 4A). Similar NREMS increases restricted to the dark phase following infection in WT mice were reported by Toth and Verhulst (2003). The AcPbKO mice maintain their sleep rhythms as observed by REMS and NREMS amounts after viral challenge, yet their temperature rhythms deteriorated earlier and to a greater extent than in WT mice (Fig 4A). Infected mice demonstrate reduced locomotor activity that is also accompanied by a loss of circadian rhythms (Conn et al 1995) this was apparent in AcPbKO mice on Day 3 several days before the reductions occurred in WT mice (Fig 4B). The time of onset and severity of these responses to mouse-adapted influenza virus

in a particular mouse strain is determined by the dose of virus administered (Conn et al 1995, Toth et al., 1995, Fang et al., 1995). Herein, we infected with a lower dose than used previously in our lab (e.g. Majde et al 2007; Leyva-Grado et al 2009; Majde et al 2010) and accordingly the observed turning point of the acute phase response was delayed by 3 days in WT mice (Fig 4).

The time courses of virus-induced NREMS EEG SWA responses and duration of NREMS are different in both WT and AcPbKO mice (Figs 3I & 3K). NREMS EEG SWA is often used as a measure of sleep intensity and sleep homeostasis. The separation of NREMS SWA from NREMS duration is exaggerated in the AcPbKO mice due to their large virus-induced reduction in NREMS EEG SWA beginning as early as PI Day 2. Such responses recapitulate the independent regulation of delta power from sleep duration (Davis et al 2011). Regardless, AcPb seems to be involved in both sleep and EEG slow wave power.

It is not known the extent to which the AcPb-associated effects on sleep are localized to specific brain regions. IL1β and its receptor increase with sleep loss in the hypothalamus, hippocampus, and cerebral cortex. Local application of IL1 to the somatosensory cortex enhances EEG NREMS SWA unilaterally and Fos immunoreactivity in associated cortical areas and hypothalamic sleep regulatory areas (Yasuda et al 2005; 2007). Further, in rats and mice SD is followed by enhanced IL1 mRNA and AcPb mRNA expressions in the somatosensory cortex (Taishi et al 1998, 2012; Zielinski et al 2012). In rats, but not mice, SD enhances hypothalamic IL1 mRNA and injection of IL1 into the hypothalamic area enhances sleep (Alam et al 2004) suggesting subcortical sites are also involved in mediating IL1-sleep effects. AcPb is also implicated in hippocampal synaptogenesis (Huang et al 2011, Yoshida et al 2012). Extended sleep deprivation compromises hippocampal neogenesis and proliferation (Guzmin-Marin 2003; Garcia-Garcia et al 2011). Recent evidence indicates that the type I IL1 receptor and glucocorticoids mitigate the detrimental effects of sleep loss on cell survival (Mueller et al 2014). This protective role could result in part from AcPb, as AcPb facilitates neuronal survival following excitotoxicity (Gosselin et al 2013). Thus the roles of IL1-signalling in brain extend beyond its classic pro-inflammatory actions including neuronal plasticity and sleep regulation. Further, the contribution of AcPb to brain functions is illustrated by its ability to activate Src kinases independent of the canonical IL1 signaling pathway via NFkB (Huang et al 2011) and its ability to act as a cell adhesion molecule (Yoshida et al 2012).

Collectively these data provide strong evidence for an important role for AcPb in host defenses and sleep regulation. Our results add to the growing evidence that AcPb is integral to multiple diverse brain functions. Further, that a neuron-specific protein profoundly affects morbidity and mortality caused by a lung disease suggests alternative approaches to treatment and perhaps prevention of influenza virus-induced disease.

Acknowledgements

References

Amadori M. The role of IFN-alpha as homeostatic agent in the inflammatory response: A balance between danger and response? J. Interferon Cytokine Res. 2007; 27:181–190. [PubMed: 17348816]

Alam MN, McGinty D, Bashir T, Kumar S, Imeri L, Opp MR, Szymusiak R. Interleukin-1beta modulates state-dependent discharge activity of preoptic area and basal forebrain neurons: role in sleep regulation. Eur J Neurosci. 2004; 20:207–216. [PubMed: 15245493]

Besedovsky L, Lange T, Born J. Sleep and immune function. Pflugers Arch. 2012; 463:121–137. [PubMed: 22071480]

Cavadini G, Petrzilka S, Kohler P, Jud C, Tobler I, Birchler T, Fontana A. TNF-alpha suppresses the expression of clock genes by interfering with E-box-mediated transcription. Proc Natl Acad Sci U S A. 2007; 104:12843–12848. [PubMed: 17646651]

Conn CA, McClellan JL, Maassab HF, Smitka CW, Majde JA, Kluger MJ. Cytokines and the acute phase response to influenza virus in mice. Am. J. Physiol. 1995; 268:R78–R84. [PubMed: 7530928]

Davis CJ, Clinton JM, Jewett KA, Zielinski MR, Krueger JM. Delta wave power: an independent sleep phenotype or epiphenomenon? J Clin Sleep Med. 2011; 7:S16–8. [PubMed: 22003323]

Fang J, Sanborn CK, Renegar KB, Majde JA, Krueger JM. Influenza viral infections enhance sleep in mice. Proc. Soc. Exp. Biol. Med. 1995; 210:242–252. [PubMed: 8539262]

Fang J, Wang Y, Krueger JM. The effects of interleukin-1β on sleep are mediated by the type I receptor. Am. J. Physiol. 1998; 274:R655–R660. [PubMed: 9530230]

Franken P, Chollet D, Tafti M. The homeostatic regulation of sleep need is under genetic control. J Neurosci. 2001; 21:2610–2621. [PubMed: 11306614]

García-García F, De la Herrán-Arita AK, Juárez-Aguilar E, Regalado-Santiago C, Millán-Aldaco D, Blanco-Centurión C, Drucker-Colín R. Growth hormone improves hippocampal adult cell survival and counteracts the inhibitory effect of prolonged sleep deprivation on cell proliferation. Brain Res. Bull. 2011; 84:252–257. [PubMed: 21256199]

Gosselin D, Bellavance MA, Rivest S. IL-1RAcPb signaling regulates adaptive mechanisms in neurons that promote their long-term survival following excitotoxic insults. Front Cell Neurosci. 2013; 7:1–12. [PubMed: 23355802]

Grimm D, Staeheli P, Hufbauer M, Koerner I, Martínez-Sobrido L, Solórzano A, García-Sastre A, Haller O, Kochs G. Replication fitness determines high virulence of influenza A virus in mice carrying functional Mx1 resistance gene. Proc. Natl. Acad. Sci. U. S. A. 2007; 104:6806–6811. [PubMed: 17426143]

Guzman-Marin R, Suntsova N, Stewart DR, Gong H, Szymusiak R, McGinty D. Sleep deprivation reduces proliferation of cells in the dentate gyrus of the hippocampus in rats. J. Physiol. 2003; 549:563–571. [PubMed: 12679377]

Huang Y, Smith DE, Ibanez-Sandoval O, Sims JE, Friedman WJ. Neuron-specific effects of interleukin-1β are mediated by a novel isoform of the IL-1 receptor accessory protein. J. Neurosci. 2011; 31:18048–18059. [PubMed: 22159118]

Huber R, Deboer T, Tobler I. Effects of sleep deprivation on sleep and sleep EEG in three mouse strains: empirical data and simulations. Brain Res. 2000; 857:8–19. [PubMed: 10700548]

Imeri L, Bianchi S, Opp MR. Inhibition of caspase-1 in rat brain reduces spontaneous nonrapid eye movement sleep and nonrapid eye movement sleep enhancement induced by lipopolysaccharide. Am J Physiol Regul Integr Comp Physiol. 2006; 291:R197–204. [PubMed: 16455762]

Imeri L, Opp MR. How (and why) the immune system makes us sleep. Nat. Rev. Neurosci. 2009; 10:199–210. [PubMed: 19209176]

Kuo TH, Williams JA. Acute Sleep Deprivation Enhances Post-Infection Sleep and Promotes Survival during Bacterial Infection in Drosophila. Sleep. 2014; 37:859–869. [PubMed: 24790264]

Krueger JM. The role of cytokines in sleep regulation. Curr. Pharm. Design. 2008; 14:3408–3416.

Krueger JM, Taishi P, De A, Davis C, Winters BD, Clinton J, Szentirmai E, Zielinski MR. ATP and the purine type 2 X7 receptor affect sleep. J. Appl. Physiol. 2010; 109:1318–1327. [PubMed: 20829501]

Leyva-Grado V, Churchill L, Wu M, Williams TJ, Taishi P, Majde JA, Krueger JM. Influenza virus- and cytokine-immunoreactive cells in the murine olfactory and central autonomic nervous systems before and after illness onset. J. Neuroimmunol. 2009; 211:73–83. [PubMed: 19410300]

Liao F, Taishi P, Churchill L, Urza JM, Krueger JM. Localized suppression of cortical growth hormone releasing hormone receptors state-specifically attenuates EEG delta waves. J. Neurosci. 2010; 30:4151–4159. [PubMed: 20237285]

Majde JA, Bohnet SG, Ellis GA, Churchill L, Leyva-Grado V, Wu M, Szentirmai E, Rehman A, Krueger JM. Detection of mouse-adapted human influenza virus in the olfactory bulb of mice within hours after intranasal infection. J. Neurovirol. 2007; 13:399–409. [PubMed: 17994424]

Majde JA, Kapas L, Bohnet SG, De A, Krueger JM. Attenuation of the influenza virus sickness behavior in mice deficient in Toll-like receptor 3. Brain Behav. Immun. 2010; 24:306–315. [PubMed: 19861156]

Majde JA, Krueger JM. Links between the innate immune system and sleep. J. Allergy Clin. Immunol. 2005; 116:1188–1198. [PubMed: 16337444]

Mueller AD, Parfyonov M, Pavlovski I, Marchant EG, Mistlberger RE. The inhibitory effect of sleep deprivation on cell proliferation in the hippocampus of adult mice is eliminated by corticosterone clamp combined with interleukin-1 receptor 1 knockout. Brain Behav. Immun. 2014; 35:102–108. [PubMed: 24121035]

Mizuguchi M, Yamanouchi H, Ichiyama T, Shiomi M. Acute encephalopathy associated with influenza and other viral infections. Acta Neurol. Scand. 2007; 115:45–56. [PubMed: 17362276]

Opp MR, Obál F Jr, Krueger JM. Interleukin-1 alters rat sleep: temporal and dose-related effects. Am. J. Physiol. 1991; 260:R52–R58. [PubMed: 1992828]

Smith DE, Lipsky BP, Russell C, Ketchem RR, Kirchner J, Hensley K, Huang Y, Friedman WJ, Boissonneault V, Plante MM, Rivest S, Sims JE. A central nervous system-restricted isoform of the interleukin-1 receptor accessory protein modulates neuronal responses to interleukin-1. Immunity. 2009; 30:817–831. [PubMed: 19481478]

Taishi P, Bredow S, Guha-Thakurta N, Obál F Jr, Krueger JM. Diurnal variations of interleukin-1β mRNA and β-actin mRNA in rat brain. J. Neuroimmunol. 1997; 75:69–74. [PubMed: 9143239]

Taishi P, Chen Z, Obál F Jr, Zhang J, Hansen M, Fang J, Krueger JM. Sleep-associated changes in interleukin-1β mRNA in the brain. J. Interferon Cytokine Res. 1998; 18:793–798. [PubMed: 9781819]

Taishi P, Churchill L, Wang M, Kay D, Davis CJ, Guan X, De A, Yasuda T, Liao F, Krueger JM. TNFα siRNA reduces brain TNF and EEG delta wave activity in rats. Brain Res. 2007; 1156:125–132. [PubMed: 17531209]

Taishi P, Davis CJ, Bayomy O, Zielinski MR, Liao F, Clinton JM, Smith DE, Krueger JM. Brain –specific interleukin-1 receptor accessory protein in sleep regulation. J. Appl. Physiol. 2012; 112:1015–1022. [PubMed: 22174404]

Taishi P, Sanchez C, Wang Y, Fang J, Harding JW, Krueger JM. Conditions that affect sleep alter the expression of molecules associated with synaptic plasticity. Am. J. Physiol. Regul. Integr. Comp. Physiol. 2001; 281:R839–845. [PubMed: 11506999]

Tobler I, Borbély AA. Sleep EEG in the rat as a function of prior waking. Electroencephalogr Clin Neurophysiol. 1986; 64:74–76. [PubMed: 2424723]

Toth LA, Jhaveri K. Sleep mechanisms in health and disease. Comp Med. 2003; 53:473–486. [PubMed: 14655989]

Toth LA, Rehg JE, Webster RG. Strain differences in sleep and other pathophysiological sequelae of influenza virus infection in naive and immunized mice. J. Neuroimmunol. 1995; 58:89–99. [PubMed: 7730450]

Toth LA, Tolley EA, Krueger JM. Sleep as a prognostic indicator during infectious disease in rabbits. Proc. Soc. Exp. Biol. Med. 1993; 203:179–192. [PubMed: 8502660]

Toth LA, Verhulst SJ. Strain differences in sleep patterns of healthy and influenza-infected inbred mice. Behav. Genet. 2003; 33:325–36. [PubMed: 12837021]

Vyazovskiy VV, Achermann P, Tobler I. Sleep homeostasis in the rat in the light and dark period. Brain Res Bull. 2007; 74:37–44. [PubMed: 17683787]

Wong JP, Saravolac EG, Clement JG, Nagata LP. Development of a murine hypothermia model for study of respiratory tract influenza virus infection. Lab. Anim. Sci. 1997; 47:143–147. [PubMed: 9150492]

Yasuda K, Churchill L, Yasuda T, Blindheim K, Falter M, Krueger JM. Unilateral cortical application of interleukin-1beta (IL1beta) induces asymmetry in fos, IL1beta and nerve growth factor immunoreactivity: implications for sleep regulation. Brain Res. 2007; 1131:44–59. [PubMed: 17184753]

Yasuda T, Yoshida H, Garcia-Garcia F, Kay D, Krueger JM. Interleukin-1beta has a role in cerebral cortical state-dependent electroencephalographic slow-wave activity. Sleep. 2005; 28:177–184. [PubMed: 16171241]

Yoshida T, Shiroshima T, Lee S-J, Yasumura M, Uemura T, Chen X, Iwakura Y, Mishina M. Interleukin-1 receptor accessory protein organizes neuronal synaptogenesis as a cell adhesion molecule. J. Neurosci. 2012; 32:2588–2600. [PubMed: 22357843]

Zielinski MR, Krueger JM. Sleep and innate immunity. Front Biosci (Schol Ed). 2011; 3:632–642. [PubMed: 21196401]

Zielinski MR, Taishi P, Clinton JM, Krueger JM. 5'-Ectonucleotidase-knockout mice lack non-REM sleep responses to sleep deprivation. Eur J Neurosci. 2012; 35:1789–1798. [PubMed: 22540145]

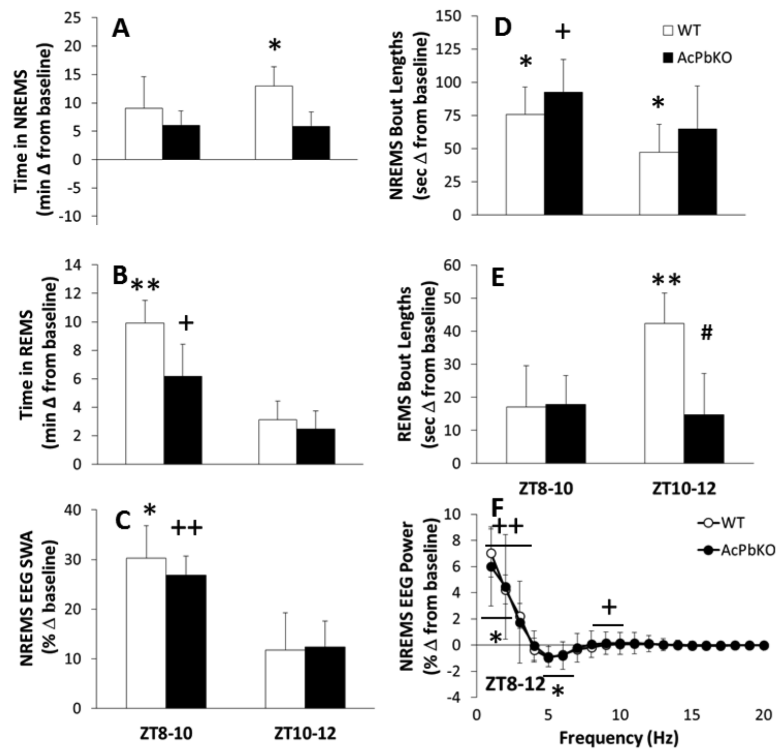**Figure 1.**
AcPbKO mice have attenuated sleep responses to sleep loss. WT and AcPbKO mice were deprived of sleep from ZT22-8 and then allowed to spontaneously sleep the next day. NREMS, REMS, NREMS EEG SWA and spectral responses for the first 4 h post-sleep deprivation (ZT8-12) are shown as difference from baseline; during this period sleep rebound responses are maximum (*p<0.05, **p<0.01, WT baseline vs. SD; +p<0.05, ++p<0.01, AcPbKO baseline vs. SD; #p<0.05 WT vs. AcPbKO).
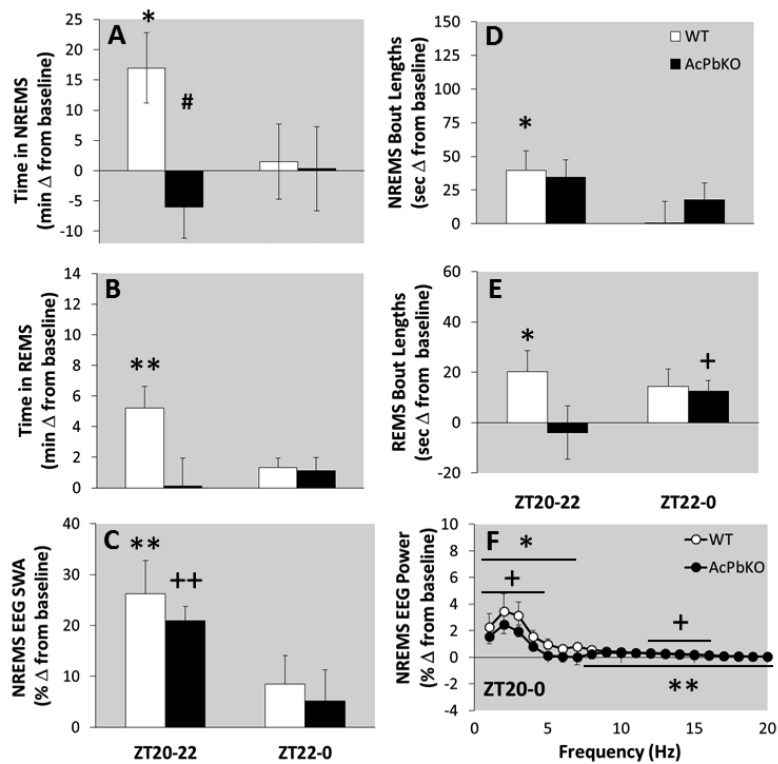
Figure 2.
AcPbKO mice lack NREMS rebound and REMS rebound is reduced compared to WT mice after sleep deprivation from ZT10-20. WT and AcPbKO mice were deprived of sleep from ZT10-20 then allowed to spontaneously sleep for the 24 h. NREMS, REMS, NREMS EEG SWA and spectral responses for the first 4 h post-sleep deprivation (ZT20-0) are shown as difference from baseline (*p<0.05, **p<0.01, WT baseline vs. SD; +p<0.05, ++p<0.01, AcPbKO baseline vs. SD; #p<0.05 WT vs. AcPbKO; shaded background indicates lights off).
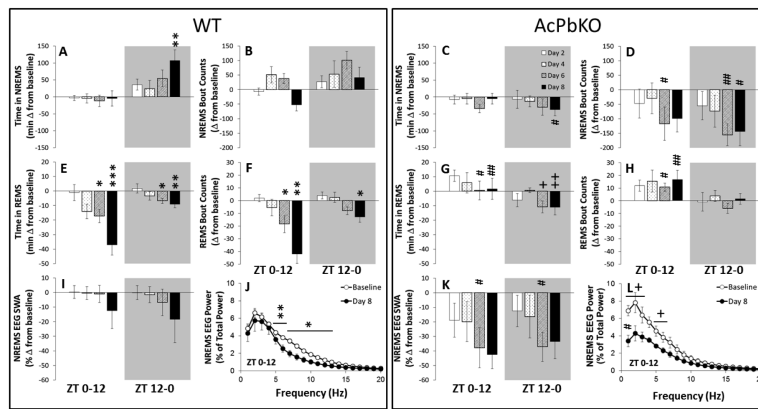
Figure 3.
AcPbKO mice have blunted sleep responses to influenza virus challenge. The AcPbKO mice had less NREMS during nighttime hours (shaded areas representing the 12 h dark period) than their corresponding baseline values. In contrast, WT mice increased NREMS during this period. REMS was inhibited on Day 8 post-viral challenge in WT mice, but not AcPbKO mice. The AcPbKO mice also had lower EEG SWA values during NREMS (*p<0.05, **p<0.01, WT baseline vs. post injection day; +p<0.05, ++p<0.01, AcPbKO baseline vs. post injection day and #p<0.05, ##p<0.01, WT vs. AcPbKO).
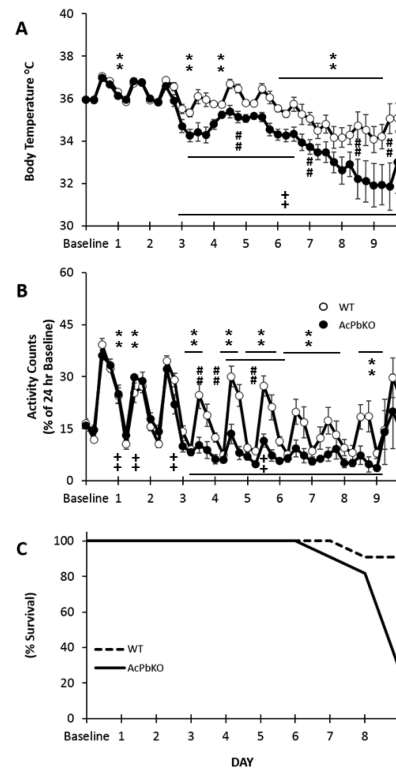
Figure 4.
AcPbKO mice are more hypothermic, less active and have higher mortality than WT mice following viral challenge. Decreased temperature and activity symptoms present on post-infection Day 3 in AcPbKO mice and post-infection Day 6 in WT mice (**$p<0.01$, WT baseline vs. post injection day; [++]$p<0.01$, AcPbKO baseline vs. post injection day ; [##]$p<0.01$ WT vs. AcPbKO).